International Journal of Nanomedicine

Dovepress
open access to scientific and medical research

Open Access Full Text Article

ORIGINAL RESEARCH

Honokiol-mesoporous Silica Nanoparticles Inhibit Vascular Restenosis via the Suppression of TGF-β Signaling Pathway

This article was published in the following Dove Press journal:
International Journal of Nanomedicine

Xiao Wei[1,*]
Zhiwei Fang[2,*]
Jing Sheng[1]
Yu Wang[3]
Ping Lu[1]

[1]Department of Geriatrics, Shanghai Ninth People's Hospital, Shanghai Jiao Tong University School of Medicine, Shanghai 200011, People's Republic of China; [2]Engineering Research Center of Cell & Therapeutic Antibody, Ministry of Education, School of Pharmacy, Shanghai Jiao Tong University, Shanghai 200240, People's Republic of China; [3]Department of Cardiology, Shidong Hospital of Yangpu District, Shanghai 200438, People's Republic of China

*These authors contributed equally to this work

Introduction: The main pathological mechanism of restenosis after percutaneous coronary intervention (PCI) is intimal hyperplasia, which is mainly caused by proliferation and migration of vascular smooth muscle cells (VSMCs). Our previous study found that honokiol (HNK), a small-molecule polyphenol, can inhibit neointimal hyperplasia after balloon injury, but its specific mechanism is still unclear. Moreover, poor water solubility as well as low bioavailability of honokiol has limited its practical use.

Methods: We used mesoporous silica nanoparticles (MSNPs) as a standard substance to encapsulate HNK and then assemble into honokiol-mesoporous silica nanoparticles, and we investigated the effect of these nanoparticles on the process of restenosis after common carotid artery injury in rats.

Results: We report a promising delivery system that loads HNK into MSNPs and finally assembles it into a nanocomposite particle. These HNK-MSNPs not merely inhibited proliferation and migration of VSMCs by reducing phosphorylation of Smad3, but also showed a higher suppression of intimal thickening than the free-honokiol-treated group in a rat model of balloon injury.

Conclusion: To sum up, this drug delivery system supplies a potent nano-platform for improving the biological effects of HNK and provides a promising strategy for preventing vascular restenosis.

Keywords: mesoporous silica nanoparticles, honokiol, vascular smooth muscle cells, TGF-β pathway, balloon injury, intimal thickening, restenosis

Introduction

Restenosis, mainly arising from intimal hyperplasia, is the re-narrowing of a blood vessel after angioplasty.[1,2] Stimulated by cytokines and inflammatory mediators, the vascular smooth muscle cells (VSMCs) change from contractile to synthetic type, excessive VSMCs proliferation in intima is the main pathological mechanism of restenosis.[3] Active synthetic VSMCs constantly proliferate, migrate and accumulate in the intima and perform repair function, then inducing vascular remodeling.[4–6] Antiproliferative agent targeting the VSMCs is the most important treatment strategy for intimal hyperplasia.[7]

Restenosis is not only caused by vascular remodeling, but also closely related to the deposition of extracellular matrix (ECM).[8] Collagen is the main component of ECM, which is secreted by synthetic VSMCs. Excessive secretion of ECM result in

Correspondence: Yu Wang; Ping Lu
Email 1300941009@qq.com; pinglushanghai@163.com

submit your manuscript | www.dovepress.com
DovePress
http://doi.org/10.2147/IJN.S250911

imbalance of collagen synthesis and degradation.[9,10] Regulating the synthesis and degradation of collagen is also a therapeutic target for intimal hyperplasia.[9]

Honokiol (HNK) is one of the main active ingredients in *Magnolia officinalis*. It has been used to treat gastrointestinal disorders, anxiety, neurological disorders and other diseases as a folk medicine for centuries.[11] Our previous study demonstrated that free-honokiol can significantly inhibit intimal thickening after common carotid artery injury in rabbits.[12] However, the underlying mechanism remains unclear, and the clinical application was hampered by physiochemical characteristics of HNK: poor stability due to the oxidation, poor water solubility, and bioavailability.[13,14] Therefore, we tried to design a nanocarrier system for HNK encapsulation and delivery to overcome these unsatisfying physicochemical properties.

The advent of nanomaterials makes it easier to transport drugs into cells. Nanomaterials can effectively increase the uptake of drugs and thus improve their efficacy, and they may reduce the toxicity and side effects of drugs through spatiotemporally controlled release. Ideal nanomaterials often have good biodegradability, biocompatibility, low toxicity, and are easy to produce.[15–19] The mesoporous structure of mesoporous silica nanoparticles (MSNPs) endows its highly uniform pore passage, large surface area, narrow pore diameter distribution, and wide range, so that MSNPs can accommodate and adsorb small molecule drugs.[20–22] MSNPs improve the solubility of drugs through physical, chemical and other interactions, and can be used to reduce the poor water-solubility of drugs.[23] MSNPs prove to be a good candidate for the present study because (i) it has a high surface area in contact with living organisms, (ii) pores of uniform size make the drug diffuse and release constantly, (iii) drug molecules can be confined in mesoporous structures thus avoiding recrystallization.[24,25] MSNPs are believed to be easily absorbed by cells and have high transmission efficiency. With the decomposition of MSNPs, encapsulated drugs could be released and the carrier fragments are easily excreted through the renal system.[17,26] Therefore, MSNPs provides an ideal platform for the delivery of small molecule drugs.

Herein we designed a delivery system of honokiol-loaded MSNPs that can successfully transport HNK into cells and improve the pharmacodynamic effects of HNK (Figure 1). We used a MSNP standard substance to encapsulate HNK and then assemble it into honokiol-mesoporous silica nanoparticles (HNK-M). Periadventitial application of HNK-M by F-127 pluronic gel demonstrated that HNK-M effectively inhibited the process of restenosis after common carotid artery injury in rats.

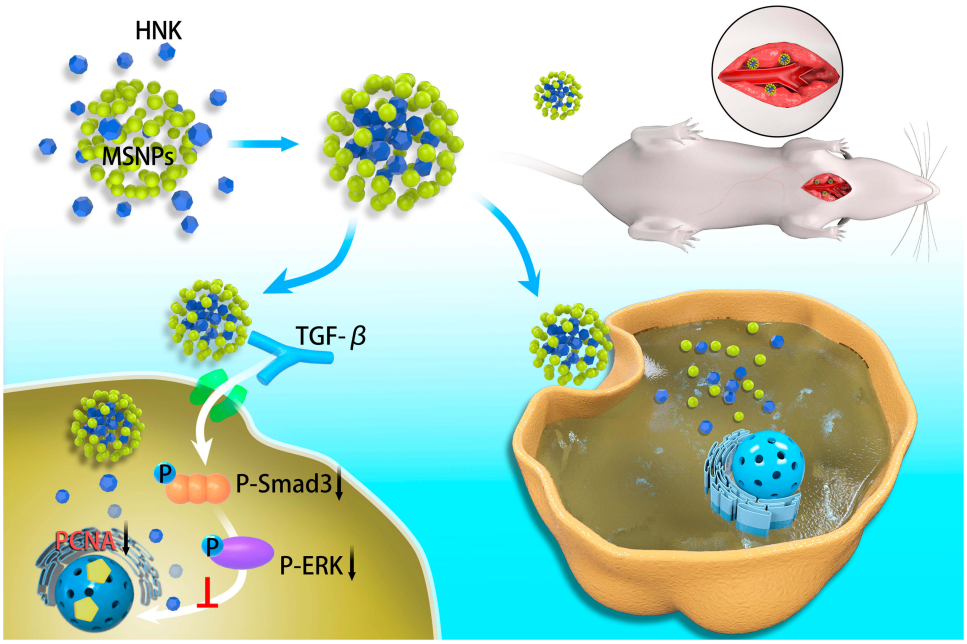

Figure 1 Schematic of honokiol-mesoporous silica nanoparticles with inhibiting proliferation and migration of VSMCs, preventing and treating restenosis after vascular injury and simultaneously inhibiting TGF-β pathway.

Materials and Methods

Materials

VSMCs were obtained from the Cell Bank of the Chinese Academy of Sciences (Shanghai, China). Honokiol was purchased from Selleck Chemicals (Houston, USA, catalog no. S2310), MSNPs (catalog no. 643645) and F-127 pluronic gel were purchased from Sigma-Aldrich Co. (St Louis, MO, USA). Transmission electron microscope was acquired from FEI (Hillsboro, Oregon, USA). FBS and 0.25% (w/v) trypsin−EDTA were obtained from Corning (New York, USA). DMEM and penicillin−streptomycin solution were purchased from Gibco (Thermo Fisher Scientific, Waltham, MA, USA). Culture flasks (25 cm^2 surface area), culture plates, a filter of 8 μm pore size and confocal dishes were acquired from Corning Incorporated (Corning, NY, USA). 2F Fogarty embolectomy catheters were obtained from Edwards Lifesciences (Irvine, CA, USA). WST-1 was purchased from Beyotime Biotechnology (Shanghai, China). Foxp3/Transcription Factor Staining Buffer Set was purchased from Thermo Fisher Scientific. The primary antibodies used in Western blotting analysis were: anti-p-smad3, anti-p-ERK1/2 and anti-PCNA (Immunoway Biotechnology, NY, USA). α-SMA antibody was obtained from Abcam (Cambridge, UK).

Ethics Statement

Animals received humane care, the experiment was approved by the Animal Care and Use Committee of Shanghai Jiao Tong University School of Medicine, animal protocols were carried out in accordance with the Animal Care and Use Committee of Shanghai Ninth People's Hospital, Shanghai Jiao Tong University School of Medicine.

Preparation of the Honokiol-loaded Mesoporous Silica Nanoparticles (HNK-M)

There are three generic drug-loading strategies for MSNPs: supercritical CO_2 technique, solvent-based methods and melting processes.[27] HNK-M were prepared using solvent-based method with modified parameters.[28] Briefly, MSNPs were sonicated and then the mixtures of free-honokiol /MSNPs (1:2 weight ratio) were dispersed in appropriate ethyl alcohol. The complex was left in a shaker for 24 h at room temperature in the dark. The HNK-M was obtained and dried with nitrogen. The residua were concentrated to uniformly disperse in moderate deionized water. When the mesoporous silica carrier decomposes, encapsulated HNK was released simultaneously. In order to protect the stability of nanoparticles, HNK-M in this study was dried and preserved in the powder form, in which case no HNK escaped or MSNP decomposition occurred.[17,29]

Characterization of the HNK-M

The morphological shapes of the prepared nanoparticles were observed by transmission electron microscope (TEM). The nanoparticles were dispersed with distilled water at 0.5 mg/mL concentration and sonicated in order to form a system with homogenous density. HNK-M was placed on a copper grid coated with carbon membrane and the grid was dried at room temperature before observation.

Cell Culture

The VSMCs were grown in DMEM containing 10% FBS, 100 IU/mL penicillin, and 100 μg/mL of streptomycin in 75-cm^2 flasks at 37°C in a humidified atmosphere of 5% CO_2.

Preparation of the Agentia-loaded Pluronic Gel

F127 hydrogels containing free-honokiol, MSNPS and HNK-M were prepared by the traditional method.[12] 0.3 g of pluronic F127 was dissolved in 1 mL saline overnight at 4°C, and then free-honokiol, MSNPs and HNK-M (contains 2 mg HNK and 4 mg MSNPs, respectively) were added and vortexed. The mixture was stored at 4°C for future use.

Cytotoxicity Assay of Free Honokiol and HNK-MSNPs

The cytotoxicity of free-honokiol and HNK-M on VSMCs was evaluated with the WST-1 cell proliferation and cytotoxicity assay kit. Briefly, cells suspensions were distributed in a 96-well plate at a density of 1×10^4 cell/well in 200 μL of standard medium for 24 h. The cells were then exposed to free-honokiol and HNK-M at different concentrations and then incubated at 37°C with 5% CO_2 for 24 h. After the appropriate incubation time, the supernatant was removed and then mixed with 20 μL of WST-1 solution. Next, the mixture was incubated at 37°C in 5% CO_2 atmosphere for 1.5 h, and the absorbance of each sample was measured at 450 nm using an automated microplate reader. The relative cell viability (%) was estimated from data of three individual experiments, and results were expressed as mean ±SD.

Flow Cytometric Analysis

The VSMCs were harvested after incubation with the drugs, washed with PBS twice, fixed and permeated using the Foxp3/Transcription Factor Staining Buffer Set. Then the cells were blocked with blocking solution containing 0.5% BSA/permeabilization buffer for 15 min, stained with the PCNA-antibody. Finally, the samples were washed twice with staining buffer and the cell proliferation assays were examined with FACS Calibur flow cytometer.

Migration Assay

For the migration assays, we used transwell inserts with a filter of 8 μm pore size. The VSMCs were cultured in serum free system for 24 h, and then 6×10^4 cells in serum-free medium were seeded into the supper chamber of the transwell insert containing free-honokiol and HNK-M. The cells were allowed to migrate toward the lower chamber. After 24-h incubation, cells in the upper part of the transwell were removed with a cotton swab, and the cells which migrated on the lower surface of inserts and were fixed by 4% paraformaldehyde and stained with 0.1% crystal violet. Filters were photographed and the total number of cells were counted from six randomly selected fields.

Western Blot Analysis

Following treatment for the indicated conditions, VSMCs and common carotid artery were washed with cold PBS and lysed in RIPA buffer. Cells and tissue were centrifuged at 12,000 rpm for five minutes, and the supernatant containing the protein was collected. The concentration of protein was determined using a BCA protein assay kit. Twenty micrograms of protein from each sample were electrophoretically separated using a 12% sodium dodecyl sulfate-polyacrylamide (SDS-PAGE) gel and were transferred to polyvinylidene fluoride (PVDF) membranes, which were blocked in 5% BSA for two hours at room temperature, followed by incubation overnight at 4°C with the primary antibodies. The following primary antibodies and dilution ratios were used: anti-p-smad3; anti-p-ERK; anti-PCNA. The membranes were rinsed and incubated for two hours at room temperature with horseradish peroxidase (HRP)-conjugated secondary antibody. The immunoreactive bands were visualized with an enhanced chemiluminescence detection kit. The relative protein levels were quantified by image-pro-plus software version 6.0 (Media Cybernetics, Inc. Rockville, Maryland USA).

Construction of Balloon Injury Model and In Vivo Drug Delivery

Common carotid artery balloon injury model was performed using a conventional method.[30] Figure 6A B Male Sprague Dawley rats (450–550 g) were anesthetized with pentobarbital sodium and an incision made in the middle of the neck. A 2-F balloon catheter was inserted into the common carotid artery through the external carotid artery, the balloon was filled with 50 μL normal saline, and then pulled three times to establish the animal model of vascular balloon injury. Immediately following balloon injury, the agentia-loaded pluronic gel was applied around the outside of the injured artery. The gel coagulated immediately at body temperature. Animals were euthanized and then the carotid arteries were collected 3, 7, 14, and 28 days post-surgery.

Immunofluorescence Staining

VSMCs were allowed to grow on the slides in conditioned culture medium. After incubation by free-honokiol, MSNPs and HNK-MSNPs (80 μM, 120 μM), the slides were washed three times in PBS, fixed in staining fix solution for 15 min, and then permeabilized with 0.5% Triton X-100 in PBS containing 1% BSA for 30 min. After washing with PBS twice, the cells were stained overnight at 4°C with Alexa Fluor 594-conjugated anti-rat PCNA antibody. The cells were then washed three times with PBS, stained with DAPI for five minutes, and observed using a confocal microscopy. In vivo, to analyze the expression of PCNA in the intima, paraffin sections of the common carotid artery were prepared and the VSMCs of intima were located with α-SMC.

Histology and Morphometry

The tissue samples were fixed in formalin solution for 24 h and then embedded in paraffin. Then, the samples were cut into 5 μm sections, stained with H&E and Masson. The tissue stained area was quantified by the Image-Pro Plus version 6.0.

Results and Discussions

Preparation and Characterization of Honokiol-loaded MSNPs (HNK-M)

MSNPs have hydrophilic surfaces and are easier to be absorbed by cells. Besides, MSNPs are acknowledged to

be one of the most promising drug-carrier systems because it can be readily removed from the body and is nontoxic. Small molecule drugs (eg, HNK in this study) were usually loaded into MSNPs by three generic strategies, ie, the molecules of HNK are embedded into dense interior of MSNPs, encapsulated in the mesoporous structure of MSNPs, or physically adsorbed on the surface of MSNPs.[17] Hydrophobic drug HNK was successfully encapsulated in hydrophilic silica nanoparticles, we evaluated the morphology and toxicity of HNK-M. Figure 2A showed a typical TEM image of HNK-M, they were spherical in shape and superimposed on top of each other. The density inside HNK-M was not uniform as a result of the presence of mesoporous interspace. The WST-1 assay was used for quantitative testing of the viability of VSMCs treated with free-honokiol, MSNPs and HNK-M. WST-1 is a compound similar to MTT and can be reduced to orange formazan by dehydrogenase in the mitochondria. It was shown that the amount of formazan dye is directly correlated to the number of living cells.[31] As shown in Figure 2B, MSNPs is almost nontoxic to VSMCs, the optimal concentration of HNK for effective therapy on VSMCs was believed to be around 100 μM. Figure 2B showed that there was no difference in toxicity between free-honokiol and HNK-M at concentrations ranging from 80 μM to 120 μM. The IC_{50} values for free-honokiol and HNK-M were 136.8 and 152.7 μM, respectively. The HNK-M compound can improve the efficacy of HNK and cellular uptake compared to the free-honokiol. These results provided that MSNPs effectively delivered the HNK to VSMCs by virtue of its preferable biocompatibility and the ability to reduce the toxicity of HNK. MSNPs-coated HNK can be transported into cells in a short time. Because of low biocompatibility, HNK cannot be transported into cells efficiently and exist in the cell matrix or culture medium for a long time, thus damaging the integrity of cell membrane. Therefore, compared with MSNPs, free-honokiol is more toxic to cells. Thus, to avoid potential interference with cell viability, the noncytotoxic concentrations of HNK (≤136.8 μM) were used in the subsequent experiments.

HNK-M Inhibits VSMC Growth In Vitro

PCNA is an accessory protein of DNA polymerase delta and is required in the synthesis of DNA during the cell cycle.[32] Thus, PCNA can be used as an indicator to evaluate cell proliferation. Flow cytometry was used to determine the expression of PCNA in VSMCs treated with free-honokiol and HNK-M respectively. As shown in Figure 3A and B, the expression of PCNA in the MSNP-treated group was similar to that in the blank control group, indicating that MSNPs have no inhibitory effect on proliferation of VSMCs. Over the same concentration range, the expression of PCNA in the free-honokiol group was 7.4% and 14.2% respectively at concentrations of 80 and 120 μM. However, the results of the HNK-M group were 17.1% and 24.5%, which were both higher than that with corresponding concentrations in the free-honokiol group. To further confirm the expression of PCNA, IF technology was utilized to detect the fluorescence intensity of PCNA in each group. As shown in Figure 3C and D, VSMCs in the control group expressed highest levels of PCNA, while free-honokiol and HNK-M groups showed a remarkably lower fluorescence intensity of PCNA. At the same concentration, the fluorescence intensity of PCNA in HNK-M group was lower than that in free-honokiol group. IF showed a similar result to that of flow cytometry. Taken together, these results suggested

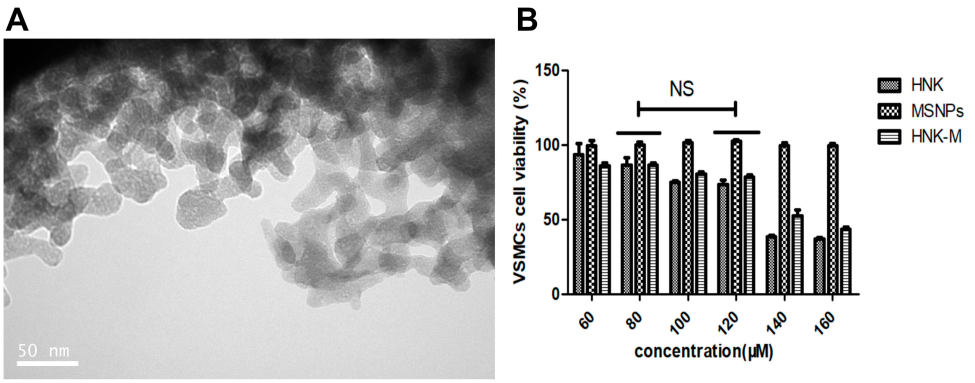

Figure 2 (**A**) Transmission electron microscopy (TEM) images of HNK-M. Scale bar: 50 nm. (**B**) Viability of Hela VSMCs incubated for 24 h with different concentrations of free-HNK, MSNPs and HNK-M. Data are given as the mean ±SD (n=3, $^{NS}P>0.05$).

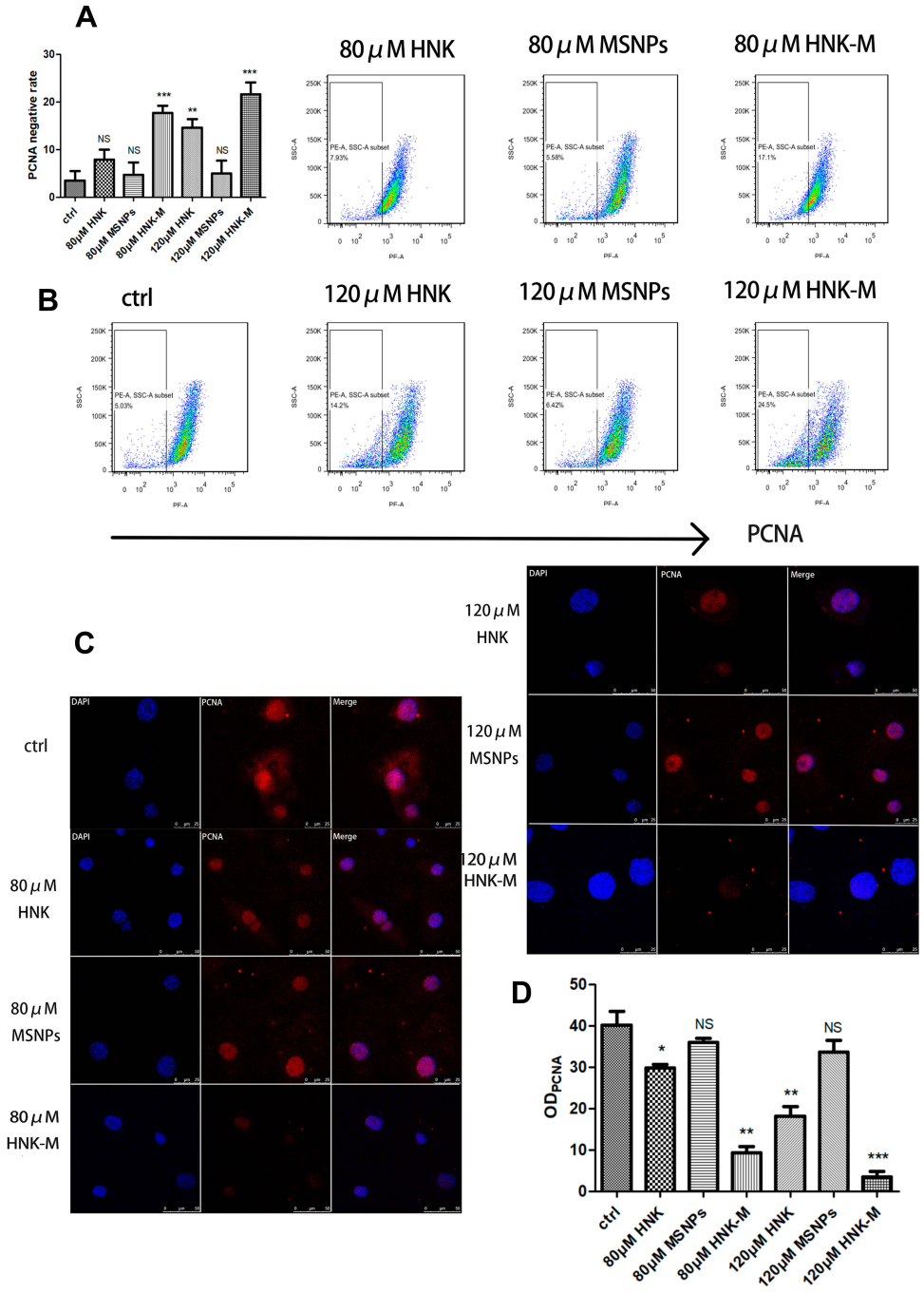

Figure 3 (**A**) Quantification of PCNA negative rate (n=3). (**B**) FACS analysis in PCNA downregulation. (**C**) Confocal laser scanning microscope images of PCNA expression in VSMCs. PCNA and cell nuclei were stained with Alexa Fluor® 594 (red) and 4,6-diamino-2-phenyl indole (DAPI) (blue), respectively. (**D**) Quantification of PCNA expression by mean fluorescence intensity (MFI). Cells were preincubated with free-HNK, MSNPs and HNK-M at a concentration of 80 μM and 120 μM. Scale bar: 50 μm. Data in (**A**) and (**D**) are given as the mean ±SD (n=3, $^{NS}P>0.05$, $^{*}P<0.05$, $^{**}P<0.01$, $^{***}P<0.001$).

that the application of MSNPs significantly increased the antiproliferative ability of honokiol on VSMCs.

HNK-M Inhibits VSMCs Migration

Migration of VSMCs to the intima is one of the mechanisms leading to restenosis after vascular injury. To test whether HNK-M can inhibit the migration of VSMCs, we performed a transwell assay on cultured VSMCs (Figure 4A). Transwell assay was carried out using a Boyden chamber. It consists of two chambers separated by a microporous membrane as a physical barrier that the cells can only overcome by active migration. As shown in Figure 4B, on the

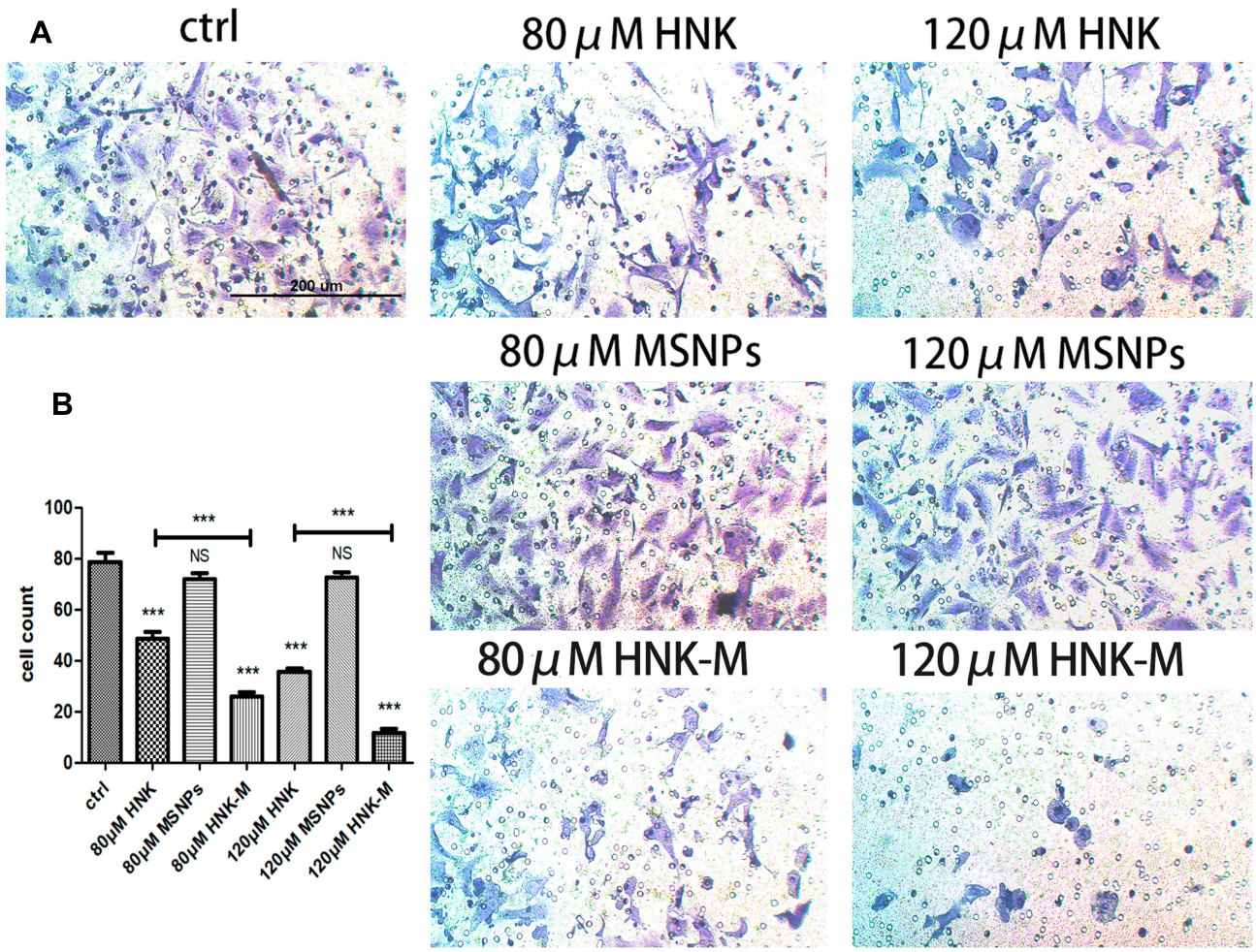

Figure 4 (**A**) Representative images of VSMCs migrated through the microporous membrane, stained with crystal violet.Original magnifications: 100 × (**B**) Quantitative analysis of cell numbers (n=6). Cells were preincubated with free-HNK, MSNPs and HNK-M. Cells without treatment were used as control. Data are given as the mean ±SD ($^{NS}P>0.05$, $^{***}P<0.001$).

average, there were 78.5 cells crossing the membrane in the control group. While in both free-honokiol and HNK-M treated groups, fewer migrating cells were observed. When compared with free-honokiol treated group, HNK-M significantly reduced the number of migrating cells at both 80 and 120 μM concentrations ($P<0.001$). These results confirmed that HNK-M can efficient inhibit VSMC migration, the application of MSNPs significantly improved the inhibiting effect of HNK on migration.

The antiproliferation and antimigration effect of HNK-M was significantly higher than that of HNK, which indicated that honokiol-loaded MSNPs that can successfully improve the pharmacodynamic effects of HNK in vitro. MSNPs supplied a potent nano-platform for the intracellular delivery of HNK to VSMCs. This was probably attributed to the reduction of poor water-solubility and controlled release.

HNK-M Downregulates Proteins Involved in TGF-β Signaling Pathway

It was found that the repair process of VSMCs could be accelerated by transforming growth factor-beta (TGF-β) through the activation of multiple intracellular signal pathways.[8,33] TGF-β is a ligand to cell surface receptor that could activate phosphorylation of smad protein in cells. Smad protein is an important regulatory molecule of TGF-β superfamily signal transduction, in which p-smad2/3 as a part of receptor-regulated smad is transported to the nucleus with the assistance of common-mediator smad (p-smad4). In the nucleus, the R-smad/Co-smad complex can initiated the PCNA gene transcription process by interacting with other nuclear cofactor proteins. Furthermore, p-smad2/3 can activate the extracellular signal-regulated kinase (ERK) pathway of mitogen-activated protein kinase (MAPK) family.[34–36] Inhibition of the TGF-

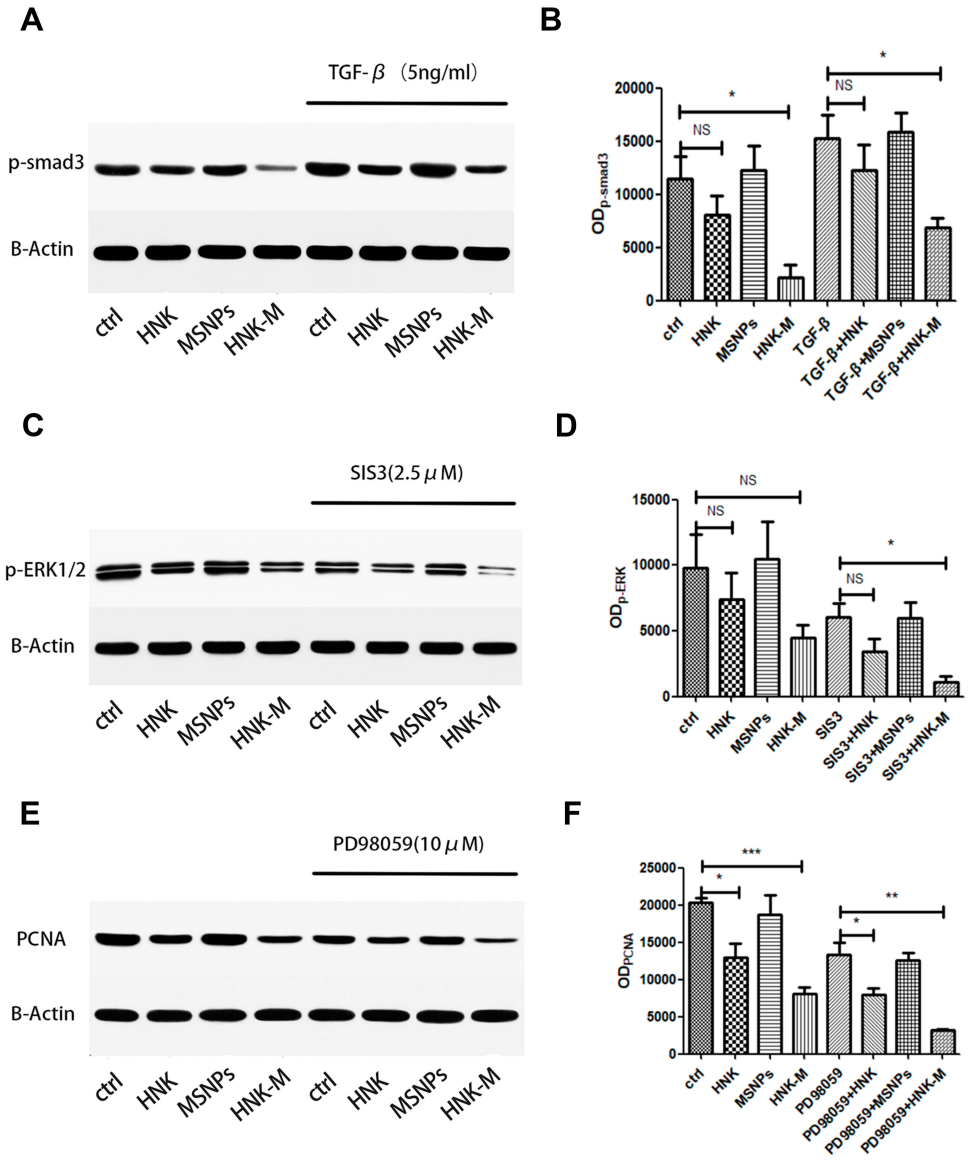

Figure 5 Western blot analysis of the p-smad3 (**A**), p-ERK1/2 (**C**) and PCNA (**E**) in VSMCs after treating with TGF-β, SIS3 and PD98059, respectively. β-Actin was used as a loading control. Quantification of p-smad3 (**B**), p-ERK1/2 (**D**) and PCNA (**F**) expression level by measuring the band density and then normalizing according to β-Actin. All data in (**B, D** and **F**) are given as the mean ± SD (n=3, $^{NS}P>0.05$, $^{*}P<0.05$, $^{**}P<0.01$, $^{***}P<0.001$).

β pathway through different means can decrease intimal hyperplasia.[34,36–38]

To evaluate the potential inhibitory effects on TGF-β signaling pathway, Western blots were performed on p-smad3 of VSMCs treated with free-honokiol, MSNPs and HNK-M. As shown in Figure 5A and B, overexpression of p-smad3 on VSMCs was observed by irritation with TGF-β (5 ng/mL) for one hour. The phosphorylation state of smad3 can be inhibited by free-honokiol and HNK-M, and the inhibitory effects of HNK-M is more obvious than that of free-HNK. Beyond that, we further evaluated the interaction of smad family and ERK pathway in VSMCs and explored whether HNK-M downregulated the expression of PCNA induced by p-ERK. VSMCs were pretreated with free-honokiol, MSNPs and HNK-M for 24 h, respectively, and then cultured with SIS3 (SIS3 is a cell-permeable and selective inhibitor of smad3) or PD98059 (PD98059 is a potent, selective and cell-permeable MEK1 and MEK2 inhibitor). The expression of p-ERK and PCNA was measured with Western blot assay. In Figure 5C–F, we confirmed that the expression of activated ERK1/2 decreased when inhibiting the phosphorylation process of smad3, and HNK-M can significantly downregulate the expression of p-ERK1/2 and PCNA compared to the free-honokiol group.

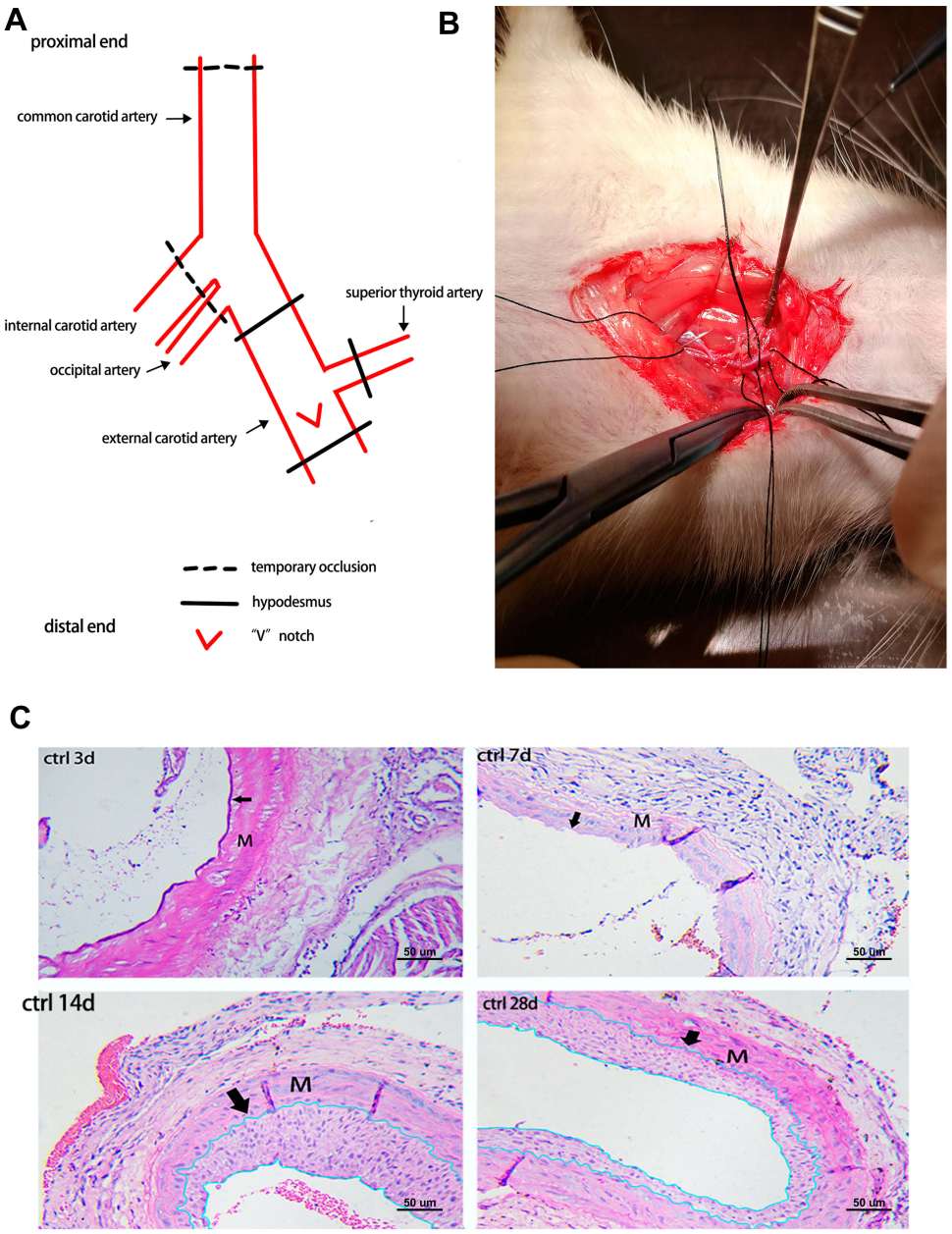

Figure 6 (**A**) Pattern of balloon injury model in rats. (**B**) Representative image of rats during the operation. (**C**) Measurement in thickness of carotid artery intima at three, seven, 14, and 28 days after balloon-injured carotid artery in rats. The black arrows indicated the boundary between intima and media area. Original magnifications: 200 ×.

HNK-M Inhibits Intimal Hyperplasia After Vascular Injury

In order to determine the point-in-time of draw materials, degree of intimal was measured after common carotid artery injury at days 3, 7, 14, and 28. As shown in Figure 6C, there was no visible hyperplasia of intima after three and seven days of vascular injury, so it was impractical to evaluate the changes of intima during this period. The new neointima was developed enough at 14 days after injury, and the neointima formation process kept at a stable state compared with 28 days, this is consistent with a previous research.[39] Hence, 14 days after carotid injury operation was set as the predetermined time point in the following study.

Intimal hyperplasia is the primary cause of restenosis after vascular injury.[40] The potential of HNK-M in prevention of restenosis after vascular injury can be preliminarily evaluated by investigating the intimal thickness. We applied an H&E staining to determine the intimal situation in this rat balloon injury model. As shown in Figure 7A, in the control group, the neointimal hyperplasia induced significant

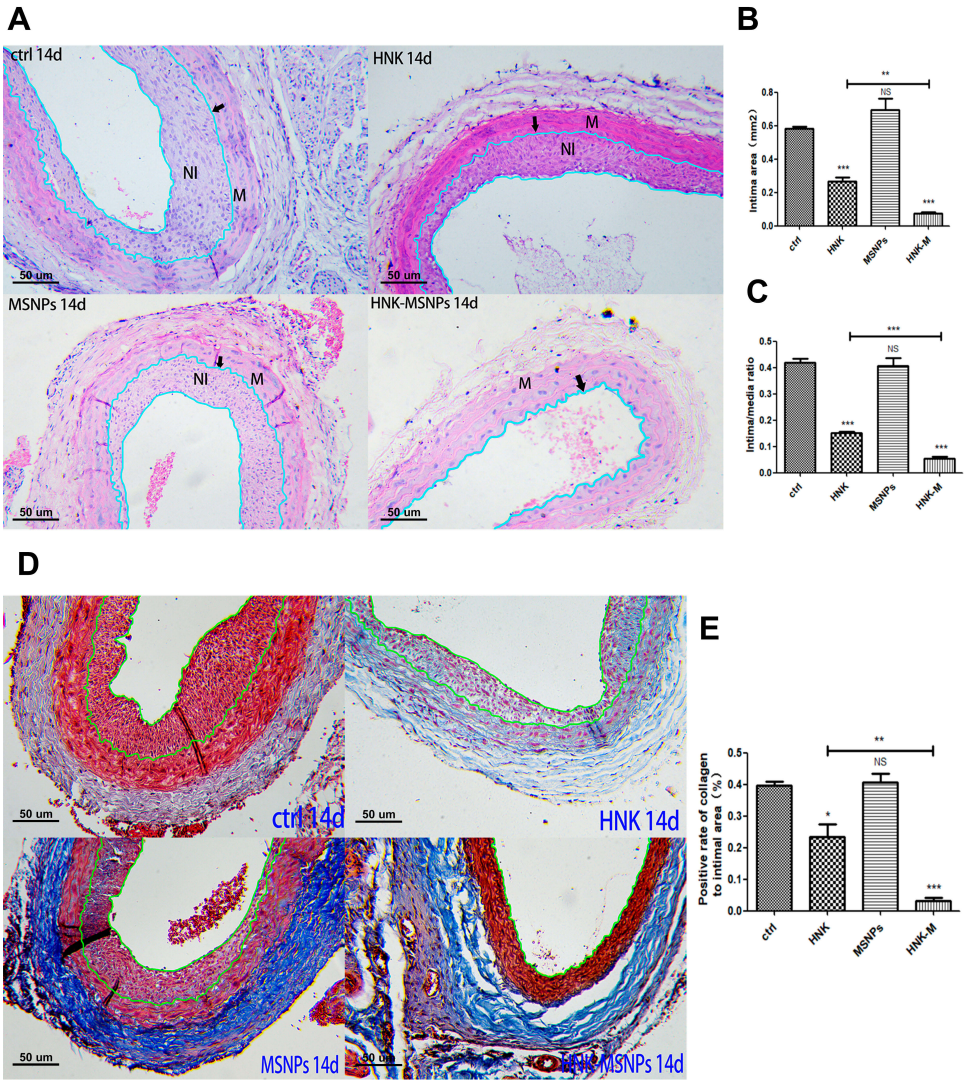

Figure 7 Therapeutic effect of HNK-M in vivo. Histological analysis of H&E (**A**) and Masson (**D**) stained sections of injured arteries 14 days after balloon angioplasty. Original magnifications: 200 ×.Quantification of average intima area (**B**) and average intima/media area ratios (**C**) for the three treatment groups and control group. (**E**) Determination of position rate of collagen to intimal area. All data in (**B, C** and **E**) are given as the mean ±SD (n=8, $^{NS}P>0.05$, $^{*}P<0.05$, $^{**}P<0.01$, $^{***}P<0.001$).

restenosis, which almost blocked the lumen. Compared with the control group, HNK-M administration could markedly inhibit the intimal hyperplasia, which was quantified by intima/media ratio and intima area. In Figure 7B and C, at 14 days, there was a 72.5% decrease in the intima area in HNK-M group treated compared with that of free-honokiol group (0.2651±0.024 vs 0.0728±0.009, P=0.0019), meanwhile, the intima/media ratio decreased by 64.5% (0.1520±0.005 vs 0.0539±0.007, P=0.0004). However, no significant differences were observed between control and MSNPs treated groups. The results indicated that HNK-M showed the best inhibitory effect on the intima hyperplasia in the vascular injury.

HNK-M Inhibits Collagen Deposition

The excessive ECM deposition leads to the formation of neointima.[9] Collagen is the main component of ECM and reducing collagen deposition is a therapeutic target for intimal hyperplasia,[9] our previously study showed that free-honokiol inhibits collagen deposition in injured carotid artery.[12] The position rate of intimal collagen was measured by Masson staining 14 days after vascular balloon injury. Figure 7D and E revealed that the deposition of collagen in vascular intima was less in the HNK-M treated group than the free-honokiol group (P<0.05), which indicated that HNK-M successfully achieved higher inhibitory effect on collagen deposition.

HNK-M Inhibits VSMCs Proliferation In Vivo

In normal vascular tissue, VSMCs have a contractile phenotype: they proliferate slowly, are functionally contractile and express a range of contractile proteins, including α-SM-actin (α-SMA).[41] We investigated whether HNK-M could suppress expression of PCNA and VSMCs proliferation in vivo. We performed immunofluorescence staining for α-SMA and PCNA, and used α-SMA to localize VSMCs in the intima. As presented in Figure 8A and B, after 14 days after injury, the immunofluorescence of the blood vessels showed that most cells in the neointima expressed α-SMA (green). PCNA expression in HNK-M treatment

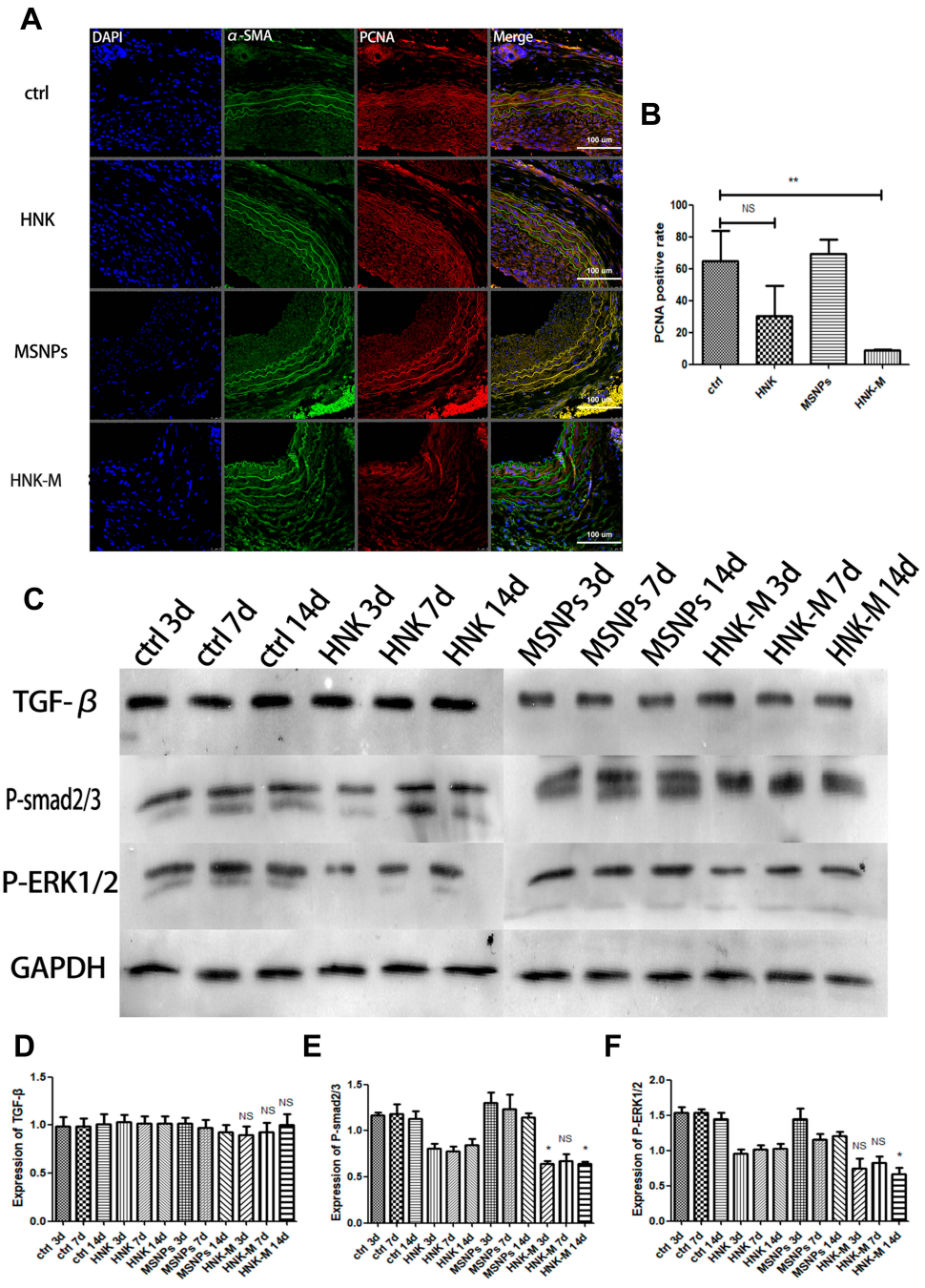

Figure 8 (**A**) Evaluation of PCNA expression (red) of VSMCs in the intima which were located with α-SMA (green). Original magnifications: 400 ×. (**B**) Quantification of PCNA expression by MFI. (**C**) Common carotid artery with balloon injury were treated with free-honokiol, MSNPs and HNK-M at predetermined time, and TGF-β, p-smad2/3 and p-ERK1/2 was measured by Western blot. Quantification of the TGF-β (**D**), p-smad2/3 (**E**) and p-ERK1/2 (**F**) protein expression by measuring the band density and then normalizing it to GAPDH. All data in (**B, D, E** and **F**) are given as the mean ±SD (n=8, $^{NS}P>0.05$, $^{*}P<0.05$, $^{**}P<0.01$).

group was significantly lower compared with free-honokiol treated group and control group (P=0.0067), and yet, there was no significant difference between the free-honokiol treated group and the control group (P=0.0898). These data suggested that HNK-M significantly reduced the proliferation ability of VSMCs compared to the free-honokiol in vivo.

HNK-M Inhibits the Conduction of the TGF-β Signaling Pathway In Vivo

TGF-β plays an important role in the regulation of a key pathological response to restenosis: intimal thickening and arterial remodeling.[42] In the in vitro study, we have demonstrated that TGF-β can stimulate the phosphorylation of smad2/3 in VSMCs, and overexpression of p-smad2/3 can also activate ERK1/2. Therefore, in in vivo experiments, we also used Western blot to evaluate the expressions of TGF-β, p-smad2/3 and p-ERK1/2 in common carotid artery after ballon-injury. As shown in Figure 8C–F, at three, seven, and 14 days after balloon injury, free-honokiol and HNK-M had no effect on the expression of TGF-β, but inhibited the expression of p-smad2/3 and p-ERK1/2, and the inhibitory effect of HNK-M was slightly stronger than that of the free-honokiol. The in vivo and in vitro results are consistent, further demonstrating that the HNK inhibits VSMCs proliferation by inhibiting the TGF-β pathway, and the inhibitory effect can be enhanced after encapsulated with MSNPs.

Conclusion

In this study, free-honokiol was encapsulated with MSNPs to get HNK-M, which could effectively deliver HNK into VSMCs and enhance the biological effects. The in vitro results showed that MSNPs was nontoxic to VSMCs and HNK-M can significantly inhibit the proliferation and migration of VSMCs. In vivo experiments showed that HNK-M can effectively inhibit the intimal thickening process after vascular balloon injury in rats, and inhibit the proliferation of VSMCs and deposition of collagen in intima. HNK-M improved the therapeutic effect of HNK both in vitro and in vivo. HNK inhibited the proliferation of VSMCs by inhibiting the conduction of TGF-β signal pathway and the phosphorylation of intracellular related proteins. Taken together, HNK-M delivery system described in this study is a promising candidate for the prevention of restenosis.

Ethics Approval and Consent to Participate

The experiment was approved by the Animal Care and Use Committee of Shanghai Jiao Tong University School of Medicine, all the animal protocols were carried out in accordance with the Animal Care and Use committee of Shanghai Ninth People's Hospital, Shanghai Jiao Tong University School of Medicine.

Acknowledgment

We appreciate assistance from the faculty of the Instrumental Analysis Center (IAC) of Shanghai Jiao Tong University.

Funding

The work was supported by the National Natural Science Foundation of China (no. 81300092). This study was also partly sponsored by the Interdisciplinary Program of Shanghai Jiao Tong University (no. YG2017MS22, and YG2017QN56) and the Translational Medicine Program of Shanghai Jiao Tong University (no. ZH2018QNA56).

Disclosure

The authors declare no conflicts of interest.

References

1. Omeh DJ, Shlofmitz E. *Restenosis*. Treasure Island (FL): StatPearls; 2020.
2. Setacci C, Castelli P, Chiesa R, et al. Restenosis: a challenge for vascular surgeon. *J Cardiovasc Surg (Torino)*. 2012;53(6):735–746.
3. Li Y, Zhang X, Gao J, Xiao H, Xu M. Increased telocytes involved in the proliferation of vascular smooth muscle cells in rat carotid artery balloon injury. *Sci China Life Sci*. 2016;59(7):678–685. doi:10.1007/s11427-016-5075-9
4. Forte A, Rinaldi B, Berrino L, Rossi F, Galderisi U, Cipollaro M. Novel potential targets for prevention of arterial restenosis: insights from the pre-clinical research. *Clin Sci*. 2014;127(11):615–634. doi:10.1042/CS20140131
5. Dzau VJ, Braun-Dullaeus RC, Sedding DG. Vascular proliferation and atherosclerosis: new perspectives and therapeutic strategies. *Nat Med*. 2002;8(11):1249–1256. doi:10.1038/nm1102-1249
6. Owens GK, Kumar MS, Wamhoff BR. Molecular regulation of vascular smooth muscle cell differentiation in development and disease. *Physiol Rev*. 2004;84(3):767–801. doi:10.1152/physrev.00041.2003
7. Habib A, Finn AV. Antiproliferative drugs for restenosis prevention. *Interv Cardiol Clin*. 2016;5(3):321–329. doi:10.1016/j.iccl.2016.02.002
8. Huang Y, Shen Z, Chen Q, et al. Endogenous sulfur dioxide alleviates collagen remodeling via inhibiting TGF-beta/Smad pathway in vascular smooth muscle cells. *Sci Rep*. 2016;6:19503. doi:10.1038/srep19503
9. Osherov AB, Gotha L, Cheema AN, Qiang B, Strauss BH. Proteins mediating collagen biosynthesis and accumulation in arterial repair: novel targets for anti-restenosis therapy. *Cardiovasc Res*. 2011;91(1):16–26. doi:10.1093/cvr/cvr012

10. Pasterkamp G, de Kleijn DP, Borst C. Arterial remodeling in atherosclerosis, restenosis and after alteration of blood flow: potential mechanisms and clinical implications. *Cardiovasc Res*. 2000;45(4):843–852. doi:10.1016/S0008-6363(99)00377-6
11. Yang B, Ni X, Chen L, et al. Honokiol-loaded polymeric nanoparticles: an active targeting drug delivery system for the treatment of nasopharyngeal carcinoma. *Drug Deliv*. 2017;24(1):660–669. doi:10.1080/10717544.2017.1303854
12. Wang Y, Zhao D, Sheng J, Lu P. Local honokiol application inhibits intimal thickening in rabbits following carotid artery balloon injury. *Mol Med Rep*. 2018;17(1):1683–1689. doi:10.3892/mmr.2017.8076
13. Yu R, Zou Y, Liu B, Guo Y, Wang X, Han M. Surface modification of pH-sensitive honokiol nanoparticles based on dopamine coating for targeted therapy of breast cancer. *Colloids Surf B Biointerfaces*. 2019;177:1–10. doi:10.1016/j.colsurfb.2019.01.047
14. Wang J, Liu D, Guan S, et al. Hyaluronic acid-modified liposomal honokiol nanocarrier: enhance anti-metastasis and antitumor efficacy against breast cancer. *Carbohydr Polym*. 2020;235:115981. doi:10.1016/j.carbpol.2020.115981
15. Jin R, Liu Z, Bai Y, Zhou Y, Chen X. Multiple-responsive mesoporous silica nanoparticles for highly accurate drugs delivery to tumor cells. *ACS Omega*. 2018;3(4):4306–4315. doi:10.1021/acsomega.8b00427
16. Su X, Chan C, Shi J, et al. A graphene quantum dot@Fe3O4@SiO2 based nanoprobe for drug delivery sensing and dual-modal fluorescence and MRI imaging in cancer cells. *Biosens Bioelectron*. 2017;92:489–495. doi:10.1016/j.bios.2016.10.076
17. Zhang S, Chu Z, Yin C, Zhang C, Lin G, Li Q. Controllable drug release and simultaneously carrier decomposition of SiO2-drug composite nanoparticles. *J Am Chem Soc*. 2013;135(15):5709–5716. doi:10.1021/ja3123015
18. Stead SO, McInnes SJP, Kireta S, et al. Manipulating human dendritic cell phenotype and function with targeted porous silicon nanoparticles. *Biomaterials*. 2018;155:92–102. doi:10.1016/j.biomaterials.2017.11.017
19. Shirin Nour NB, Imani R, Rabiee N, Khodaei M, Alizadeh A, Moazzeni SM. Bioactive materials: a comprehensive review on interactions with biological microenvironment based on the immune response. *J Bionic Eng*. 2019;16:563–581. doi:10.1007/s42235-019-0046-z
20. Yuan P, Mao X, Chong KC, et al. Simultaneous Imaging of endogenous survivin mRNA and on-demand drug release in live cells by using a mesoporous silica nanoquencher. *Small*. 2017;13(27):1700569. doi:10.1002/smll.201700569
21. Bollu VS, Barui AK, Mondal SK, et al. Curcumin-loaded silica-based mesoporous materials: synthesis, characterization and cytotoxic properties against cancer cells. *Mater Sci Eng C Mater Biol Appl*. 2016;63:393–410. doi:10.1016/j.msec.2016.03.011
22. Castillo RR, Baeza A, Vallet-Regi M. Recent applications of the combination of mesoporous silica nanoparticles with nucleic acids: development of bioresponsive devices, carriers and sensors. *Biomater Sci*. 2017;5(3):353–377. doi:10.1039/C6BM00872K
23. Maleki A, Kettiger H, Schoubben A, Rosenholm JM, Ambrogi V, Hamidi M. Mesoporous silica materials: from physico-chemical properties to enhanced dissolution of poorly water-soluble drugs. *J Control Release*. 2017;262:329–347. doi:10.1016/j.jconrel.2017.07.047
24. Croissant JG, Fatieiev Y, Almalik A, Khashab NM. Mesoporous silica and organosilica nanoparticles: physical chemistry, biosafety, delivery strategies, and biomedical applications. *Adv Healthc Mater*. 2018;7(4):1700831.
25. Sabio RM, Meneguin AB, Ribeiro TC, Silva RR, Chorilli M. New insights towards mesoporous silica nanoparticles as a technological platform for chemotherapeutic drugs delivery. *Int J Pharm*. 2019;564:379–409. doi:10.1016/j.ijpharm.2019.04.067
26. Rabiee N, Yaraki MT, Garakani SM, et al. Recent advances in porphyrin-based nanocomposites for effective targeted imaging and therapy. *Biomaterials*. 2020;232:119707. doi:10.1016/j.biomaterials.2019.119707
27. Amirala Bakhshian Nik HZ, Razavi S, Mohammadi H, et al. Smart drug delivery: capping strategies for mesoporous silica nanoparticles. *Microporous Mesoporous Mater*. 2020;299:110115. doi:10.1016/j.micromeso.2020.110115
28. Chen X, Wo F, Jin Y, Tan J, Lai Y, Wu J. Drug-porous silicon dual luminescent system for monitoring and inhibition of wound infection. *ACS Nano*. 2017;11(8):7938–7949. doi:10.1021/acsnano.7b02471
29. Navid Rabiee MB, Kiani M, Ghadiri AM. Rosmarinus officinalis directed palladium nanoparticle synthesis: investigation of potential anti-bacterial, anti-fungal and Mizoroki-Heck catalytic activities. *Adv Powder Technol*. 2020.
30. Shi X, Chen G, Guo LW, et al. Periadventitial application of rapamycin-loaded nanoparticles produces sustained inhibition of vascular restenosis. *PLoS One*. 2014;9(2):e89227. doi:10.1371/journal.pone.0089227
31. Peruzynska M, Cendrowski K, Barylak M, et al. Comparative in vitro study of single and four layer graphene oxide nanoflakes - Cytotoxicity and cellular uptake. *Toxicol in Vitro*. 2017;41:205–213. doi:10.1016/j.tiv.2017.03.005
32. Wu CH, Chen CW, Chen HC, Chang WC, Shu MJ, Hung JS. Elucidating the inhibitory mechanisms of magnolol on rat smooth muscle cell proliferation. *J Pharmacol Sci*. 2005;99(4):392–399. doi:10.1254/jphs.FP0050473
33. Khan R, Agrotis A, Bobik A. Understanding the role of transforming growth factor-beta1 in intimal thickening after vascular injury. *Cardiovasc Res*. 2007;74(2):223–234. doi:10.1016/j.cardiores.2007.02.012
34. Kingston PA, Sinha S, David A, Castro MG, Lowenstein PR, Heagerty AM. Adenovirus-mediated gene transfer of a secreted transforming growth factor-beta type II receptor inhibits luminal loss and constrictive remodeling after coronary angioplasty and enhances adventitial collagen deposition. *Circulation*. 2001;104(21):2595–2601. doi:10.1161/hc4601.099405
35. Suwanabol PA, Seedial SM, Shi X, et al. Transforming growth factor-beta increases vascular smooth muscle cell proliferation through the Smad3 and extracellular signal-regulated kinase mitogen-activated protein kinases pathways. *J Vasc Surg*. 2012;56(2):446–454. doi:10.1016/j.jvs.2011.12.038
36. Smith JD, Bryant SR, Couper LL, et al. Soluble transforming growth factor-beta type II receptor inhibits negative remodeling, fibroblast transdifferentiation, and intimal lesion formation but not endothelial growth. *Circ Res*. 1999;84(10):1212–1222. doi:10.1161/01.RES.84.10.1212
37. Wang Y, Zhao D, Wei X, Ma L, Sheng J, Lu P. PEGylated polyethylenimine derivative-mediated local delivery of the shSmad3 inhibits intimal thickening after vascular injury. *Biomed Res Int*. 2019;2019:8483765.
38. Sun Y, Ye P, Wu J, et al. Inhibition of intimal hyperplasia in murine aortic allografts by the oral administration of the transforming growth factor-beta receptor I kinase inhibitor SD-208. *J Heart Lung Transplant*. 2014;33(6):654–661. doi:10.1016/j.healun.2014.02.020
39. Park YJ, Min SK, Min SI, Kim SJ, Ha J. Effect of imatinib mesylate and rapamycin on the preformed intimal hyperplasia in rat carotid injury model. *Ann Surg Treat Res*. 2015;88(3):152–159. doi:10.4174/astr.2015.88.3.152
40. Razuvaev A, Lund K, Roy J, Hedin U, Caidahl K. Noninvasive real-time imaging of intima thickness after rat carotid artery balloon injury using ultrasound biomicroscopy. *Atherosclerosis*. 2008;199(2):310–316. doi:10.1016/j.atherosclerosis.2007.11.035
41. Durham AL, Speer MY, Scatena M, Giachelli CM, Shanahan CM. Role of smooth muscle cells in vascular calcification: implications in atherosclerosis and arterial stiffness. *Cardiovasc Res*. 2018;114(4):590–600. doi:10.1093/cvr/cvy010
42. Suwanabol PA, Kent KC, Liu B. TGF-beta and restenosis revisited: a Smad link. *J Surg Res*. 2011;167(2):287–297. doi:10.1016/j.jss.2010.12.020